NOISE REDUCTION USING FILTERS ON TURN-BY-TURN LHC ORBITS TO OBTAIN MAGNETIC ERRORS WITH THE ACTION AND PHASE JUMP ANALYSIS METHOD

A.C. García B., J.F. Cardona, Universidad Nacional de Colombia*, Bogotá, Colombia

Abstract

The Action and Phase Jump analysis had been successfully used to obtain magnetic errors in RHIC. Analyses in LHC encountered significant noise. In this paper, a dual band-pass filter on LHC simulated orbits to reduce the noise is discussed. Gaussian and Uniform noise are studied independently. Results show that the best filter has a bandwidth of 0.0174 around the two transverse tunes. A low-pass band filter was also used to get the closed-orbit.

INTRODUCTION

The measurement of magnetic errors in an accelerator is an important task during the commissioning. One of the methods used to localize, to measure, and to correct magnetic errors is the Action and Phase Jump (APJ) Analysis. It is based on the theoretical principle of preservation of the Action and Phase variables in absence of a magnetic error. This method had been successfully tested in RHIC using closed-orbit data from experiments [1] and its theoretical development is fully presented in [2].

Preliminary analyses on turn-by-turn (TBT) orbits at the LHC show promising results [3, 4], but with a certain levels of noise than for the RHIC case, due to a bigger bandwidth of the LHC BPMs. Efforts to reduce the noise, like taking advantage of the thousands of turns provided by the LHC BPMs system (in contrast with the few orbits used in RHIC) have been done.

In this paper we discuss the use of pass-band digital filters to reduce noise in LHC TBT orbits; supplemented by an initial change of the PYTHON APJ code. A simulation of the beam trajectory, using MAD-X, is made for the thin LHC injection optics (V.6.5), where normal and skew linear quadrupole errors A_1 and B_1 were included, at the IR quadrupole MQXA.3L5 of beam 1.

Noise originated from the distribution of particles in the beam and noise originated from the misaligments of the BPMs are simulated using a Gaussian distribution and an Uniform distribution, respectively. The BPMs gain is also taking into account by using these distributions. This type of distributions had been used in noise studies for the closed-orbit measurement [5].

A BAND-PASS FILTER FOR THE LHC

The BPMs are the devices that provides measurements of the beam position in the transverse plane around the accelerator. For a fixed longitudinal position, the transverse position is sampled every turn leading to:

$$z(n) = \sqrt{2J_z\beta_{z,BPM}}\sin\left(\psi_{z,BPM} + 2\pi Q_z n - \delta_z\right) \quad (1)$$

where $z = \{x, y\}$ is the transverse plane coordinate, J_z is the Action, $\beta_{z,BPM}$ and $\psi_{z,BPM}$ are the beam β_z-function and phase advance at the BPM longitudinal position, δ_z is the Phase, and Q_z is the accelerator tune, at the transverse plane $z = \{x, y\}$. In this study, the data simulated with MAD-X on the acelerator LHC beam 1, is used to created new trajectories with simulated noise.In one case, the noise corresponds to a Gaussian distribution of $\sigma_{Gauss} = 0.1$ mm, which is added randomly to the each BPM data, and in the other case a Uniform distribution up to 0.3 mm is used. Then the resulting signal is filtered to evaluate wheter the filter help to reduce the uncertainty on the determination of magnetic errors using APJ method.

In this study, the filter was implemented using directly PYTHON functions, although trials were also made with own built transfer functions. From the available filters, the band-pass filter was chose, because it reduces the noise without damaging the magnetic error recovery. A second order filter is implemented, with Butterworth coefficients and the double run function [6].

Table 1: Frequencies Values for the Filter Bands. The overlapping is removed.

N.	$\omega_{pass}I$ [2π rad]	$\omega_{stop}I$ [2π rad]	$\Delta\omega$ [2π rad]	$\omega_{pass}II$ [2π rad]	$\omega_{stop}II$ [2π rad]
0	0.28025	0.28075	0.0005	0.30875	0.30925
1	0.28	0.281	0.001	0.3085	0.3095
...	...	...	...	...	...
25	0.01	0.49	0.48	0.01	0.49

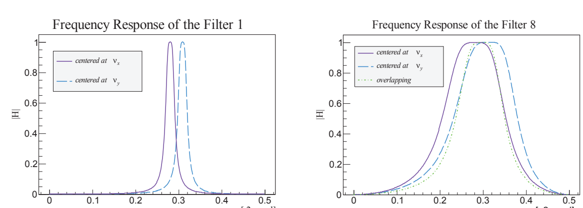

Figure 1: Dual Band-pass filter frequency response, if there is not overlapping (left) and with the corresponding overlapping band (right). Bands centered at 0.2805 and 0.309.

Also previous trials showed that the best results are obtained using a band-pass filter with two bands centered on the transverse tunes ν_x and ν_y (a 99% uncertainty is reached if only one tune band is used without noise). Table 1 presents the frequencies (ω) used to built the filter, where (N.) is the number of the case, the dots are the complementary values, such as an increment of 0.0005 in $\Delta\omega$ is

* Thanks to the DIB at Universidad Nacional de Colombia for the funding provided for computers and the support for this presentation.

ISBN 978-3-95450-138-0

always made. The band centered at ν_x corresponds to the ω labeled with I, while the band for ν_y is labeled II. The bandwidth of the two bands are the same.

The filtered signal is the addition of the signals obtained with the two single band-pass filters, whose frequency response looks like Fig. 1.left, and in case of overlapping, the addition of the filtered signals is followed by the subtraction of a band-pass signal with the overlapping frequencies as the band, the frequency response looks like Fig. 1.right.

CHANGE IN THE APJ CODE

The phase obtained from the BPM measurements (eq.(14) in [2]) is implemented with the appropriate sign in the APJ computer code, in order to count on the four quadrants of a Cartesian coordinate. This and the fact that the trajectory function has a sinusoidal behavior allow to select 2 maximal and 2 minimal (i.e. negative maximal) orbits, for each transverse plane, and not only 1 as before.

The selection of the orbits is such as the final orbit has a maximum amplitude at the error position. As reported in [3] the selection is based on the phase of the trajectory. In this study the information from the two transverse planes is necessary, therefore 8 orbits are obtained, and the phase dispersion is 0.15 rad. Each orbit, called a formable orbit, is the average of the TBT orbits that have the maximum.

Also, an initial reformulation of the error position estimation is done in the PYTHON APJ code. The transverse error position is taken as:

$$z_{error} = \sqrt{2\bar{J}_0\beta_{z,error}}\sin\left(\psi_{z,error} - \bar{\delta}_0\right) \qquad (2)$$

where $\bar{J}_0$ and $\bar{\delta}_0$ are the average of the Action and Phase in a region before the error (generally the arc before the IR), respectively, and $\beta_{z,error}$ and $\psi_{z,error}$ are the beam β-function and phase advance, at the longitudinal position of the magnetic error, respectively.

To obtain the magnetic errors A_1 and B_1, the APJ uses the relations reported at [4] or [2]. Including different combinations of the orbits, new relations are obtained as reported in the *Appendix* of this paper. For more precise and exact results an implementation of a 2D independent fit is done. This allows to get A_1 and B_1 directly from:

$$\theta_x = -xB_1 + yA_1 \quad \text{and} \quad \theta_y = xA_1 + yB_1 \qquad (3)$$

where θ is the kick produced by the error, x and y are the estimate coordinates of the trajectory at the error. This is assuming that there is not other type of magnetic error.

RESULTS AND DISCUSSION

Figure 2 contains the beam y-trajectory in the frequency space for one BPM of the LHC. Four signals are plotted in the same axis, the FFT of: the simulated, with noise, and filtered, trajectories. This representation allows to observe how the amplitude of the noise signal is reduced in the filtered signals. The difference of the noise type used implies a higher amplitude of noise for the Gaussian case, observed as well in the plane x. This contrast the fact that the Gaussian distribution has a $\sigma_{Gauss} = 0.1$ mm while the Uniform distribution is up to 0.3 mm. [1].

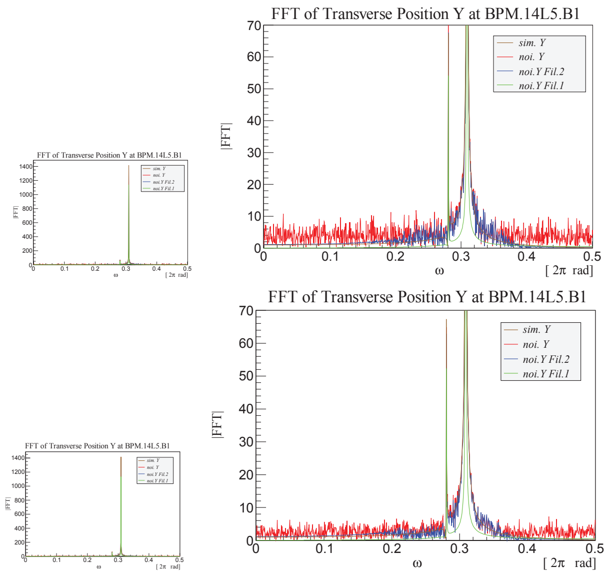

Figure 2: FFT of the Vertical Positions at BPM.14L5.B1 after 2000 turns, with Gaussian (top) and Uniform (bottom) noise. The left plots are the complete spectrumwhile the right plots is a close-up for the bottom of the spectra. All are a superimpose of a simulated (sim.) trajectory, a sim. with noise added (noi.), and a noise filtered signal for the cases N.1 (Fil. 1) and N.8 (Fil. 2) on Table 1.

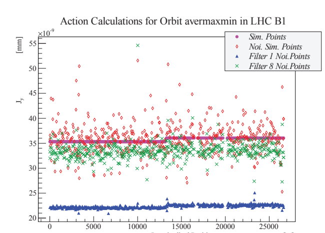

Figure 3: Action (J) along the LHC ring for one orbit type. Obtained from the simulation, without noise (Sim.), with Gaussian Noise (Noi. Sim.), and the filters N.1 and N.8 on Table 1. The magnetic errors are at 13271 m.

The Action (J) and Phase (δ) are modified with the presence of noise. Figure 3 contains J against s, without noise, for Gaussian noise and filtered, for y. The value of J is affected after the use of the filter Fil N.1, due to the difference of the trajectories amplitudes explained by the Frequency response of Fig. 1 (left). The Phase for the same orbit is in Fig. 4a. For both variables in x or y, the filter reduce the dispersion of their values. Something similar occurs with uniform noise, Fig. 5a shows δ against s, for the same type of orbit that is analyzed before, and the observations are the

[1] For both noise distributions, the BPMs resolution of 0.3 mm is the reference [7]. Because the beam distribution is Gaussian, we assumed that it is less probable to have particles of the bunche extremes affecting the BPM signal, therefore it is enough to have $\sigma_{Gauss} = 0.1$ mm.

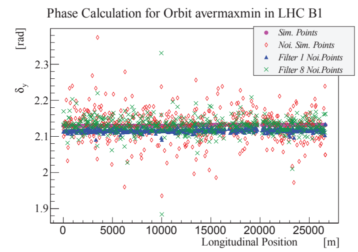

Figure 4a

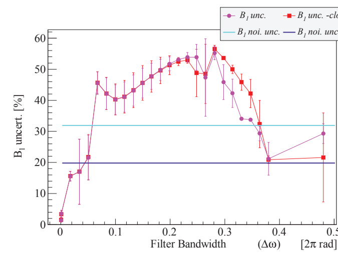

Figure 4b

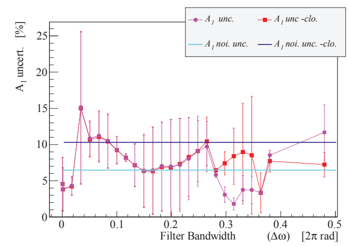

Figure 4c

Figure 4: Results for Gaussian Noise. Figure 4a contains the Phase (δ) along the LHC for the cases discussed in Fig. 3. The Uncertainty (uncert.) for B_1 and A_1 are showed in Fig. 4b and Fig. 4c, respectively, for the different bandwidths. The uncert. for the noised orbit is plotted as a horizontal line. A Low-pass filter to get the closed-orbit implies the -clo results.

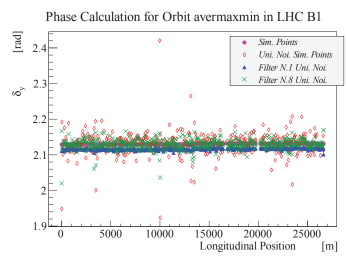

Figure 5a

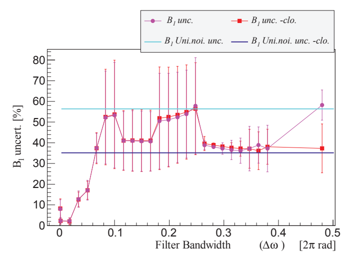

Figure 5b

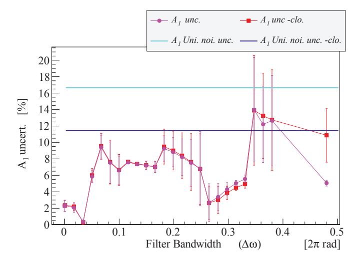

Figure 5c

Figure 5: Results for Uniform Noise in the same quantities as Fig. 4. Figure 5a contains δ while Fig. 5b and Fig. 5c contain the Uncertainty of B_1 and A_1. In the plots the precision and exactness is clearly lost for very small $\Delta\omega$.

same. Comparing the two distributions, the uniform noise implies a less dispersion.

To obtain A_1 and B_1, the selection of orbits implies that 8 points are available for the fit of Eq. 3. The magnetic errors uncertainty (taked as the Absolute Error of the measurements) of the two values obtained from the fit of Eq. 3., obtained from the fit with its dispersion (error bars), is plotted in figures Fig. 4b, Fig. 4c, Fig. 5b and Fig. 5c, against $\Delta\omega$.

Results using a low-pass band filter ($\omega_{cut} = 0.075$) for the closed-orbit calculation are reported with the line labeled as -clo. In the others, the closed-orbit is the average of the TBT trajectories. When there is noise at many frequencies, a discrepancy on the results is observed.

Also, the noise distribution affects the magnetic components in a different way. The horizontal lines, which are the uncertainty average on noised orbits (no filter used), have different values in Fig. 4b, Fig. 4c, Fig. 5b and Fig. 5c. The precision change according $\Delta\omega$ and the error.

The lesser uncertainty value for B_1 and A_1 with Gaussian and Uniform noise is obtained when $\Delta\omega = 0.0174$. This bandwidth has also a very high precision in the Uniform noise results. Diference on the noise reduction at the different bandwidths at the middle region could be corrected by setting an overlapping bandwith higher than the common ω values. In here, we are interested to take the lesser bandwidth that gives the lesser uncertainty.

CONCLUSION

A dual band-pass filter with a bandwidth of 0.0174 around the transverse tunes can be use to highly decrease Gaussian and Uniform noise in LHC orbits, when measure A_1 and B_1 at the same quadrupole using the APJ method as presented. Differences on how the closed-orbit is calculated are observed when there is noise at many frequencies.

APPENDIX

To obtain the magnetic errors, Equations (21) in [2] are used for every orbit. Other possibility is taking two orbits $(x^{(1)}, y^{(1)}, \theta_x^{(1)}, \theta_y^{(1)})$ and $(x^{(2)}, y^{(2)}, \theta_x^{(2)}, \theta_y^{(2)})$ to obtain one error, for example for B_1:

$$B_{1,x}=\frac{\theta_x^{(1)} y^{(2)} - \theta_x^{(2)} y^{(1)}}{x^{(2)} y^{(1)} - x^{(1)} y^{(2)}} \text{ and } B_{1,y}=\frac{\theta_y^{(1)} x^{(2)} - \theta_y^{(2)} x^{(1)}}{y^{(1)} x^{(2)} - y^{(2)} x^{(1)}} \tag{4}$$

The precision reached in this way is not as good as the presented results, but it could imply a faster and good measurement.

REFERENCES

[1] Javier Cardona, et. al, EPAC'04, Lucerne, TUPLT182, p.1553.

[2] Javier F. Cardona and Stephen G. Peggs, Phys. Rev. ST AB. 12 10988-4402, 2009 and Erratum 059901, 2010.

[3] J. Cardona, et. al, IPAC'11, San Sebas., WEPC004, p.2004.

[4] O.R. Blanco, et. al, PAC'11, New York, TUODN6, p.1.

[5] M. Aiba, et. al. EPAC'08, Genoa, 2008, WEPP025, p. 2572.

[6] SciPy Reference Guide (PYTHON). Functions *filtfilt*, *butter*. Pag 330-352. 2009.

[7] LHC Design Report: Vol 1 ch. 2, Geneva, CERN, 2009.

ISBN 978-3-95450-138-0